

Learning Successive Interference Cancellation for Low-Complexity Soft-Output MIMO Detection

Benedikt Fesl and Fatih Capar

Bridgecom Semiconductors

Email: benedikt.fesl@tum.de, fatih.capar@bc-s.com

Abstract—Low-complexity multiple-input multiple-output (MIMO) detection remains a key challenge in modern wireless systems, particularly for 5G reduced capability (RedCap) and internet-of-things (IoT) devices. In this context, the growing interest in deploying machine learning on edge devices must be balanced against stringent constraints on computational complexity and memory while supporting high-order modulation. Beyond accurate hard detection, reliable soft information is equally critical, as modern receivers rely on soft-input channel decoding, imposing additional requirements on the detector design. In this work, we propose recurSIC, a lightweight learning-based MIMO detection framework that is structurally inspired by successive interference cancellation (SIC) and incorporates learned processing stages. It generates reliable soft information via multi-path hypothesis tracking with a tunable complexity parameter while requiring only a single forward pass and a minimal parameter count. Numerical results in realistic wireless scenarios show that recurSIC achieves strong hard- and soft-detection performance at very low complexity, making it well suited for edge-constrained MIMO receivers.

Index Terms—MIMO detection, low-complexity, machine learning, successive interference cancellation, soft decoding.

I. INTRODUCTION

MIMO detection remains a fundamental building block of modern wireless receivers, directly impacting spectral efficiency, reliability, and energy consumption [1]. With the emergence of IoT devices and RedCap terminals, such as those specified in 5G NR, the design of MIMO detectors faces increasingly stringent constraints on computational complexity, memory footprint, and power consumption. In these scenarios, receivers are often expected to operate with limited hardware resources while still supporting moderate-to-high modulation orders and providing reliable soft information for channel decoding. At the same time, the growing interest in deploying artificial intelligence (AI) and machine learning at the physical layer, including on-device and edge-AI processing, has been explicitly recognized within 3rd Generation Partnership Project (3GPP) standardization activities [2], [3]. This motivates the development of lightweight, low-complexity, and interpretable learning-based MIMO detection algorithms that are compatible with practical receiver architectures and standardization.

From a classical signal processing perspective, MIMO detection is governed by a well-known performance-complexity trade-off. maximum likelihood (ML) detection achieves optimal performance but entails exponential complexity in the number of transmit layers and constellation size, rendering it impractical for most real-world systems. Sphere decoding (SD) [4]

approximates ML detection by restricting the search space, but the complexity remains highly variable and prohibitive, particularly for high-order modulation and unfavorable channel conditions. A large body of work has therefore focused on reducing and controlling the complexity of SD, including K-Best [5], list-SD [6], fixed-complexity SD [7], repeated and single tree search methods [8], [9], and smart candidate adding techniques [10]. While these approaches can provide high-quality soft information, their implementation complexity and memory requirements often exceed what is feasible for IoT and RedCap devices.

Alternatively, linear detectors such as zero-forcing (ZF) and minimum mean square error (MMSE) equalization offer low complexity and predictable runtime, but suffer from significant performance degradation in non-overdetermined MIMO configurations and at high modulation orders. SIC techniques, including the V-BLAST architecture [11], improve upon linear detection by exploiting layer-wise interference cancellation. However, classical SIC-based receivers are highly sensitive to error propagation and typically rely on simplistic approximations for soft-output generation, leading to limited reliability when combined with modern soft-input channel decoders such as low-density parity-check (LDPC).

Motivated by these limitations, numerous learning-based MIMO detectors have been proposed. Direct mapping methods use deep neural networks (NNs) to map received signals to transmitted symbols [12], [13], but often require large models and provide limited structural guarantees, complicating deployment on resource-constrained devices. Learning-aided SD retains ML-inspired tree search while incorporating data-driven components, including learned radius selection [14], [15], deep path prediction [16], and learned soft detection [17]; however, their reliance on explicit tree search leads to data-dependent and irregular complexity.

Model-driven and unfolding-based approaches have emerged as a promising compromise between performance and complexity. By unrolling iterative detection algorithms into trainable NNs, these methods preserve the physical structure of classical receivers while enabling data-driven optimization [18]–[23]. DeepSIC [24] and its extensions [25]–[27] employ deep NNs to perform multi-user SIC. These approaches rely on iterative refinement of symbol estimates over multiple network evaluations, resulting in increased latency and a parameter count that typically scales with the number of iterations and users, which may limit suitability for edge deployment. Interference is

mitigated implicitly through soft refinement rather than through explicit inter-layer interference cancellation, and soft information is obtained without an explicit approximation of bit-wise log-likelihood ratios (LLRs), which can reduce interpretability and robustness for downstream channel decoding.

Finally, box decoding [28] reflects the trend toward specialized low-complexity detector designs for 5G RedCap and IoT; however, its soft-output capabilities and complexity tuning granularity are comparatively limited.

In contrast to the aforementioned methods, this paper proposes *recurSIC*, a learning-based MIMO detection framework explicitly designed for low complexity and minimal memory footprint. The proposed approach builds upon the structure of classical SIC, preserving the recursive and interpretable detection principle, while enhancing each detection stage through learned lightweight modules. Unlike purely data-driven detectors, *recurSIC* is physics-informed and operates on a transformed signal model obtained via QR decomposition (QRD). In contrast to classical SIC, *recurSIC* provides explicit symbol probability estimates at each stage, enabling principled soft-output generation. Furthermore, *recurSIC* naturally extends to a multi-path formulation with a tunable complexity parameter, allowing a performance-complexity trade-off without increasing model size or re-running the detection model. The main contributions of this work are summarized as follows:

- We propose *recurSIC*, a lightweight, physics-informed, learning-based MIMO detection framework that preserves the recursive structure and low complexity of SIC.
- We introduce a multi-path extension of *recurSIC* that enables reliable soft-output detection by tracking a small and fixed number of symbol hypotheses per layer, resulting in tunable complexity and near-ML performance.
- We design a shallow NN architecture with shared weights across detection stages and signal-to-noise ratios (SNRs), yielding a minimal and constant memory footprint suitable for IoT and RedCap devices.
- Through simulations in realistic 5G NR scenarios, we demonstrate that *recurSIC* achieves strong hard-decision performance at very low complexity and provides high-quality soft information for LDPC decoding, outperforming conventional linear and classical SIC-based baselines.

II. SYSTEM MODEL AND ML DETECTION

Consider a MIMO system with L transmit layers and N receive antennas. After cyclic prefix removal and Fourier transform, the received signal per subcarrier and orthogonal frequency division multiplexing (OFDM) symbol is given as

$$\mathbf{y} = \mathbf{H}\mathbf{s} + \mathbf{n} \in \mathbb{C}^N \quad (1)$$

where $\mathbf{H} \in \mathbb{C}^{N \times L}$ denotes the effective channel, including the impact of transmit precoding, $\mathbf{s} \in \mathcal{S}_M^L$ is the transmit symbol vector drawn from an M -ary complex constellation $\mathcal{S}_M \subset \mathbb{C}$, and $\mathbf{n} \sim \mathcal{N}_{\mathbb{C}}(\mathbf{0}, \sigma^2 \mathbf{I})$ is additive white Gaussian noise (AWGN) with the SNR defined as $\text{SNR} = 1/(\sigma^2 L)$.

After QRD, e.g., of the extended channel matrix $\mathbf{H}_{\text{ext}} = [\mathbf{H}^T, \sigma \mathbf{I}]^T = \mathbf{QR}$, we get the preprocessed received signal

$\tilde{\mathbf{y}} = \mathbf{Q}^H \mathbf{y}$ [29]. The objective is to find an estimate $\hat{\mathbf{s}}$ of the transmit symbol vector \mathbf{s} . Under common assumptions, the ML solution is given by

$$\hat{\mathbf{s}}_{\text{ML}} = \arg \min_{\mathbf{s} \in \mathcal{S}_M^L} \|\tilde{\mathbf{y}} - \mathbf{R}\mathbf{s}\|^2 \quad (2)$$

which can be obtained via SD when the search radius is sufficiently large.

III. LEARNING SUCCESSIVE INTERFERENCE CANCELLATION

The proposed *recurSIC* detector is a learning-based MIMO detection framework that builds upon the structure of classical SIC. The central idea is to retain the recursive, layer-wise detection principle of SIC, which is well known for its low and predictable complexity, while enhancing each detection stage through data-driven learning. To this end, *recurSIC* consists of a sequence of lightweight NN blocks that operate in a successive manner, each producing symbol probability estimates per transmit layer. Between consecutive stages, hard symbol decisions and interference cancellation are performed, closely mirroring the structure of conventional SIC receivers.

After preprocessing the channel via QRD, $\mathbf{H} = \mathbf{QR}$, and projecting the received signal as $\tilde{\mathbf{y}} = \mathbf{Q}^H \mathbf{y} \in \mathbb{C}^L$, detection proceeds recursively over the layers $\ell = L, \dots, 1$. In this work, we employ QRD of the extended channel, cf. Section II, with the detection order determined by the largest diagonal entry $|R_{L,L}|$. Note, however, that the proposed *recurSIC* framework is agnostic to the specific choice of QRD and ordering strategy and can be readily combined with alternative preprocessing and ordering schemes. At each stage, the input to the *recurSIC* block is formed according to the classical SIC relation

$$\tilde{s}_\ell = \frac{1}{R_{\ell,\ell}} \left(\tilde{y}_\ell - \sum_{i=\ell+1}^L R_{i,\ell} \hat{s}_i \right), \quad \ell = L, \dots, 1, \quad (3)$$

where $\hat{s}_i, i = \ell+1, \dots, L$, denotes the previously detected symbols of already processed layers. This yields a layer-wise observation that accounts for residual interference and noise.

A. Single-Path *recurSIC*

In its simplest form, *recurSIC* operates with a single hypothesis per detection stage ($K = 1$). The *recurSIC* block processes the scalar input $\tilde{s}_\ell \in \mathbb{C}$ and outputs an estimate of the symbol probability vector $\hat{\mathbf{p}}_\ell \in [0, 1]^M$ over the modulation alphabet \mathcal{S}_M . A hard decision $\hat{s}_\ell = \mathcal{Q}(\hat{\mathbf{p}}_\ell)$ is obtained by selecting the constellation point with the highest estimated probability, after which the detected symbol is canceled from the received signal according to (3). This procedure is carried out sequentially throughout the layers. This single-path formulation preserves the low complexity and linear scaling of classical SIC, while benefiting from learned, layer-wise processing.

B. Multi-Path *recurSIC* for Enhanced Soft Information

While the single-path *recurSIC* already provides soft information in the form of symbol probabilities, they are of limited reliability. Greedy per-layer symbol selection based

on locally most probable hypotheses fails to fully capture the inter-layer dependencies inherent to MIMO detection, such that symbol combinations that are not locally most probable at a given layer may still be jointly optimal. This behavior is well known from ML-achieving techniques such as list-SD [6] and K-Best [5] detection. To obtain reliable soft information while simultaneously improving hard-detection performance, we extend recurSIC to a multi-path variant. Unlike classical SIC receivers that rely on linear equalization and only produce a single symbol estimate per layer, recurSIC provides explicit symbol probability estimates at each detection stage. This enables the simultaneous tracking of multiple symbol hypotheses without re-running the detection model. Specifically, we introduce a set of the K_ℓ most probable detection paths per layer ℓ . While K_ℓ can, in principle, be chosen individually for each layer, we adopt a uniform setting $K_\ell = K$ for all $\ell = 1, \dots, L$ in this work for simplicity.

For each $k = 1, \dots, K$, a symbol hypothesis $\hat{s}_\ell^{(k)} = \mathcal{Q}_k(\hat{p}_\ell)$ corresponding to the k -th most probable constellation point is selected from the symbol probability vector and propagated through an independent SIC recursion. The resulting set of hypotheses is then passed to the subsequent detection stage, effectively forming a tree of candidate symbol combinations. Owing to the data-aided and learned nature of the recurSIC stages, only a small number of paths is required in practice to obtain reliable soft information. Consequently, the proposed multi-path recurSIC tracks a fixed and limited number of hypotheses per layer within a single forward pass, achieving a favorable and predictable performance-complexity trade-off. An overview of the recurSIC framework is shown in Fig. 1 illustrates the recurSIC framework for the example case of $L = 2$ layers. The employed recurSIC blocks are NNs with a specifically designed lightweight architecture, described in detail in Section III-D, while training and inference are presented in the following.

During training, the recurSIC model is optimized using the minimum average cross-entropy over all considered symbol combinations as loss function. This formulation encourages the network to assign high probability mass to symbol hypotheses that are jointly consistent across layers, rather than optimizing each layer independently. During inference, the final hard-decision estimate is selected from the set of candidate paths generated by the multi-path recursion. Specifically, among the K^L candidate symbol vectors $\{\hat{s}_\kappa\}_{\kappa=1}^{K^L}$, the best path is chosen according to the minimum Euclidean distance

$$\hat{s}^* = \arg \min_{\kappa=1, \dots, K^L} \|\tilde{\mathbf{y}} - \mathbf{R}\hat{s}_\kappa\|^2, \quad (4)$$

which corresponds to a ML decision under AWGN, see (2).

The soft information is obtained by approximating the bit-wise LLRs using the max-log approximation. For a given transmit layer ℓ and bit position b , the LLR is computed as

$$\mathcal{L}_{\ell,b} = \min_{\hat{s} \in \mathcal{A}_{\ell,b}^{(0)}} \|\tilde{\mathbf{y}} - \mathbf{R}\hat{s}\|^2 - \min_{\hat{s} \in \mathcal{A}_{\ell,b}^{(1)}} \|\tilde{\mathbf{y}} - \mathbf{R}\hat{s}\|^2, \quad (5)$$

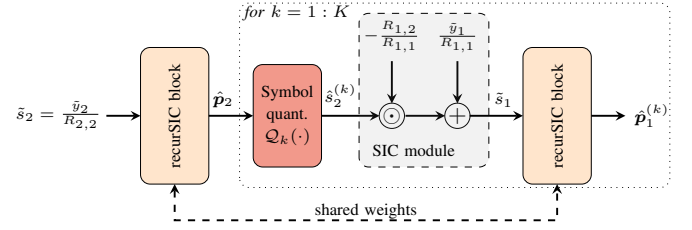


Fig. 1. Multi-path recurSIC framework for $L = 2$ layers with the recurSIC block architecture detailed in Fig. 2 and the SIC module implementing (3).

where $\mathcal{A}_{\ell,b}^{(0)}$ and $\mathcal{A}_{\ell,b}^{(1)}$ denote the sets of candidate symbol vectors for which the b -th bit of layer ℓ equals 0 and 1, respectively. In the proposed multi-path recurSIC, these sets are approximated by the collection of symbol vectors obtained from the tracked detection paths.

For small values of K , it may occur that no valid counter-hypothesis exists for a given bit b within the set of tracked paths. In this case, a fallback mechanism is employed to ensure finite and well-behaved LLR values. Starting from the best path \hat{s}^* , a counterhypothesis is constructed by flipping bit b at layer ℓ while keeping all remaining bits identical. Among the resulting symbol candidates, the one with the highest probability according to the symbol probability vector \hat{p}_ℓ is selected and used as a surrogate counterhypothesis in (5).

C. LLR Clipping

To ensure stable and well-calibrated soft outputs, the computed LLRs are subject to scaling and clipping, which is a well-known technique [6], [9]. Since recurSIC produces raw LLRs that are not explicitly scaled by the noise variance, the absolute LLR values are clipped to a maximum magnitude \mathcal{L}_{\max} , which is selected per channel model and modulation order but kept constant across SNRs. In practice, \mathcal{L}_{\max} is chosen as twice the 95th percentile of the obtained LLR distribution, which can be reliably estimated from the training set or via a simple tracking module at the receiver.

LLRs obtained via the fallback single bit-flip mechanism, i.e., counterhypotheses not contained in the tracked path set, are treated more conservatively. These LLRs are first scaled by a fixed factor $\alpha = 0.2$ to reduce their influence and then clipped in magnitude to ε_{\max} , where $\varepsilon_{\max} = 0.1 \mathcal{L}_{\max}$. This strategy limits overconfident soft information arising from incomplete hypothesis coverage while preserving the sign of the LLRs for reliable decoder operation.

D. Lightweight Network Architecture with SNR Embedding

Each recurSIC block, detailed in Fig. 2, is implemented using a lightweight NN architecture tailored to low-complexity and memory-constrained receivers. The network consists of two fully-connected hidden layers with rectified linear unit (ReLU) activations, followed by a linear output layer with softmax activation that produces the symbol probability estimates. The input to each recurSIC block is a scalar \tilde{s}_ℓ at the current detection stage, where the real and imaginary components are stacked to form a real-valued input vector.

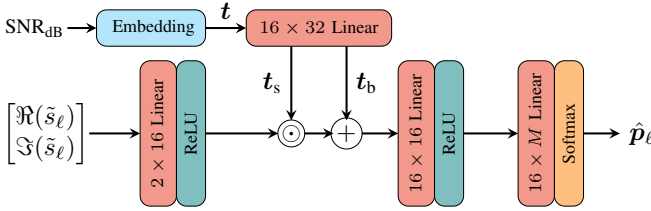


Fig. 2. NN architecture of the recurSIC block with SNR embedding. The NN parameters are shared across all detection stages and SNRs.

This low-dimensional representation is sufficient due to the structured nature of the SIC recursion and the physics-informed formulation of the detection problem.

Importantly, a single recurSIC block is trained and reused across all detection stages and SNRs, yielding a constant and minimal memory footprint independent of both the number of transmit layers and the operating SNR. To this end, a sinusoidal position embedding of the SNR information, similar to [30], is utilized to yield t , cf. [31] for details, which is, after going through a linear layer, subsequently split into a scaling vector t_s and a bias vector t_b .

IV. NUMERICAL RESULTS

For the generation of training and test datasets, the MATLAB 5G Toolbox is used to simulate a realistic 5G-NR PDSCH transmission. The training dataset comprises 200,000 samples, obtained from randomly selected resource elements across 1,000 time slots and an SNR range of [10, 30] dB. As performance metrics, we evaluate the uncoded bit error rate (BER) to assess hard-decision detection performance, as well as the block error rate (BLER) using a 3GPP-compliant LDPC decoder using normalized min-sum algorithm without retransmission and a target code-rate of 0.5 and 0.6 for 16QAM and 64QAM, respectively, to quantify the quality of the soft information, i.e., the LLRs. All results are averaged over 1,000 OFDM slots. All evaluations are performed for a 2×2 MIMO configuration, representing a non-overdetermined system model that is particularly relevant for 5G RedCap deployments.

A. Memory and Complexity Analysis

The computational complexity and memory footprint of recurSIC are summarized in Table I. Due to the model-aided, layer-wise detection structure and the use of shared weights, a single lightweight NN is employed across all detection stages and SNRs, resulting in a minimal parameter count of approximately 10^3 and $2 \cdot 10^3$ for 16QAM and 64QAM, respectively. The overall complexity scales primarily linearly with the constellation size M , as only the output dimension of the NN changes with the modulation order, while all hidden layers remain of constant size, see Fig. 2. In practical terms, this yields approximately 10^3 and $2 \cdot 10^3$ multiply-accumulates (MACs) per recurSIC block evaluation, cf. Fig. 1, for 16QAM and 64QAM, respectively. This ultra-low complexity and lightweight design stands in sharp contrast to common learning-based detectors requiring NNs with millions of parameters and

TABLE I
COMPLEXITY ORDER, PARAMETER COUNT, AND MACS OF RECURSIC

Complexity order	#Parameters	#MACs (per recurSIC block)
$\mathcal{O}(MK^{L-1})$	$864 + 17M$	$816 + 16M$

iterative evaluations, highlighting the suitability of recurSIC for edge-oriented and resource-constrained MIMO receivers.

B. Baseline Approaches

We compare against the SD with an infinite search radius, which achieves the ML solution and thus yields a performance bound. We further consider the linear MMSE equalizer, where soft information is obtained by scaling of the equalized symbols using the post-equalization SNR. In addition, we include the MMSE- and ZF-based variants of the classical SIC algorithm. Their detection order is determined by the highest post-equalization SNR at each stage.

C. TDL-A Channel

First, we consider a tapped delay line (TDL)-A channel model with Doppler frequency of 5 Hz, a delay spread of 30 ns, and medium MIMO correlation, as defined by 3GPP. For LLR clipping, cf. Section III-C, we used $\mathcal{L}_{\max} = 1.7$ and $\mathcal{L}_{\max} = 0.12$ for 16QAM and 64QAM, respectively.

The top plot in Fig. 3 shows the hard-detection performance in terms of BER for 16QAM. Already for $K = 1$, recurSIC significantly outperforms the MMSE equalizer and performs close to MMSE-SIC, while $K = 2$ yields performance approaching the ML solution, with diminishing gains for larger K in uncoded detection.

The bottom plot in Fig. 3 depicts the relative throughput ($1 - \text{BLER}$) achieved with soft-input LDPC decoding. Although the MMSE-SIC and ZF-SIC variants show improved BER over MMSE, they exhibit inferior BLER performance, particularly at high SNR, due to error propagation and overconfident LLR approximations inherent to classical SIC. In contrast, recurSIC already outperforms all non-optimal baselines for $K = 1$, and increasing K consistently enhances soft-detection performance, with $K = 8$ approaching the ML benchmark. These results demonstrate the strong hard- and soft-detection performance of recurSIC and its tunable performance-complexity trade-off, with soft decoding benefiting most from multi-path detection.

Fig. 4 presents the results for the TDL-A channel with 64QAM modulation. The qualitative behavior in terms of hard-detection performance closely mirrors the 16QAM case, with recurSIC achieving near-ML BER for small values of K . For soft-output detection, larger values of K are required compared to 16QAM, where $K \in \{6, 8, 10\}$ consistently yield improved throughput and approach the ML benchmark. These results confirm the scalability of recurSIC to higher-order modulation, with a moderate increase in the number of tracked paths.

D. TDL-B Channel

In the subsequent evaluation, we consider a TDL-B channel model with a delay spread of 100 ns and a maximum Doppler

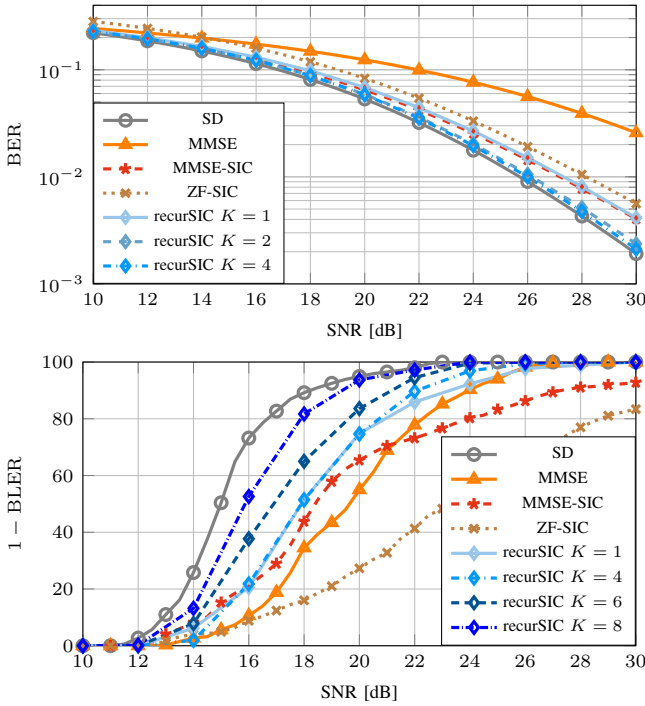


Fig. 3. Performance over TDL-A30 channel with 16QAM. Top: uncoded BER (hard-decision); bottom: relative throughput ($1 - \text{BLER}$) using soft-output.

frequency of 111.1 Hz, following the same 3GPP NR channel modeling framework as in the previous section. For LLR clipping, cf. Section III-C, we used $\mathcal{L}_{\max} = 2.4$ and $\mathcal{L}_{\max} = 0.3$ for 16QAM and 64QAM, respectively.

In Fig. 5 (top), the hard-detection performance in terms of BER is shown for the more challenging TDL-B channel. Compared to the TDL-A case, the performance gap between the linear MMSE detector and the ML benchmark is noticeably larger due to the increased delay spread and Doppler frequency. Accordingly, recurSIC benefits from larger values of K , with performance improvements visible up to $K = 6$, where near-ML performance is achieved, followed by diminishing returns.

The bottom plot of Fig. 5 presents the corresponding soft-output detection results. While $K = 1$ exhibits degraded BLER performance under the increased channel dynamics, similar to classical SIC-based approaches, recurSIC with $K \in \{4, 6, 8\}$ achieves substantial gains, consistently outperforming linear MMSE and approaching the ML benchmark. These results demonstrate the robustness and flexibility of recurSIC under more challenging fading conditions.

A similar trend is observed for the TDL-B channel with 64QAM in Fig. 6. Despite the increased channel selectivity and higher constellation order, recurSIC maintains strong hard- and soft-detection performance with moderate values of K , demonstrating its robustness and low-complexity suitability for challenging fading conditions.

V. CONCLUSION

The proposed recurSIC model learns a structured SIC process using lightweight NN blocks with shared weights

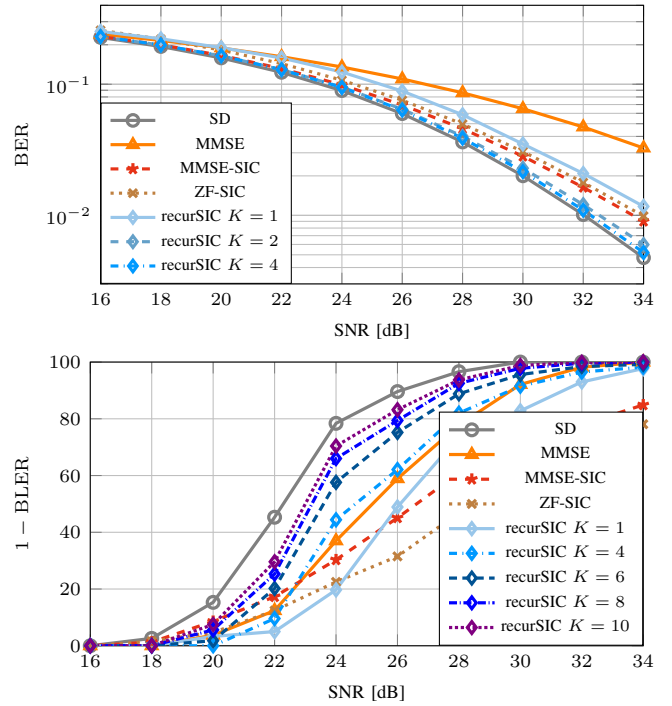


Fig. 4. Performance over TDL-A30 channel with 64QAM. Top: uncoded BER (hard-decision); bottom: relative throughput ($1 - \text{BLER}$) using soft-output.

across detection stages and positional SNR embeddings, enabling excellent generalization across noise levels at very low complexity. This design naturally supports path tracking and accurate LLR approximation, yielding both hard- and soft-output performance close to ML detection with a tunable performance-complexity trade-off. As a result, recurSIC is well suited for IoT, RedCap, and edge-oriented MIMO receivers where efficiency and reliability are critical.

Future work may explore adaptive path management, including path truncation across detection layers, effectively reducing the complexity order to $\mathcal{O}(MK)$, and per-layer selection of K to further optimize the performance-complexity trade-off and enable scalability to higher MIMO configurations, as well as joint learning of detection ordering to further mitigate error propagation.

REFERENCES

- [1] S. Yang and L. Hanzo, "Fifty years of MIMO detection: The road to large-scale MIMOs," *IEEE Commun. Surv. Tuts.*, vol. 17, no. 4, pp. 1941–1988, 2015.
- [2] 3GPP, "Study on enhancement for data collection for NR and EN-DC," 3rd Generation Partnership Project (3GPP), Tech. Rep. 37.817 (V17.0.0), Apr. 2022.
- [3] —, "Study on artificial intelligence (AI)/machine learning (ML) for NR air interface," 3rd Generation Partnership Project (3GPP), Tech. Rep. 38.843 (V19.0.0), Sep. 2025.
- [4] E. Viterbo and J. Boutros, "A universal lattice code decoder for fading channels," *IEEE Trans. Inf. Theory*, vol. 45, no. 5, pp. 1639–1642, 1999.
- [5] Z. Guo and P. Nilsson, "Algorithm and implementation of the K-best sphere decoding for MIMO detection," *IEEE J. Sel. Areas Commun.*, vol. 24, no. 3, pp. 491–503, 2006.
- [6] B. Hochwald and S. ten Brink, "Achieving near-capacity on a multiple-antenna channel," *IEEE Trans. Commun.*, vol. 51, no. 3, pp. 389–399, 2003.

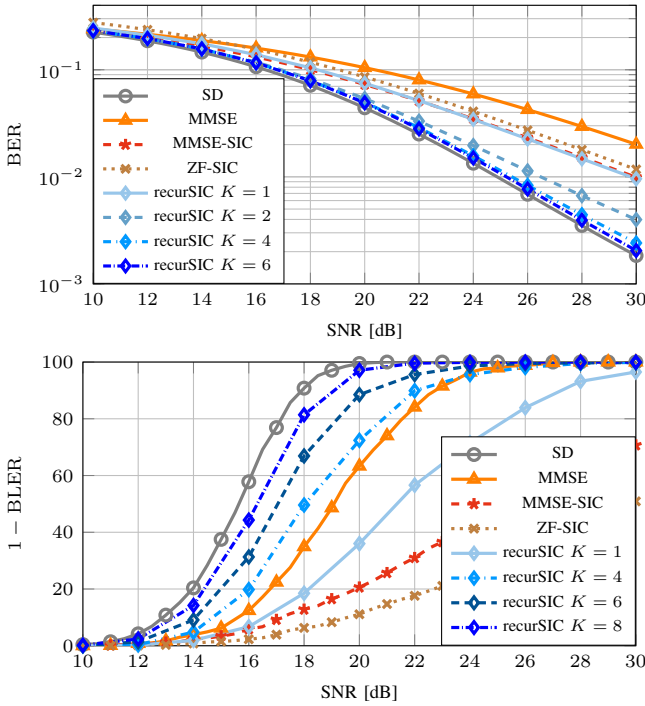


Fig. 5. Performance over TDL-B100 channel with 16QAM. Top: uncoded BER (hard-decision); bottom: relative throughput ($1 - \text{BLER}$) using soft-output.

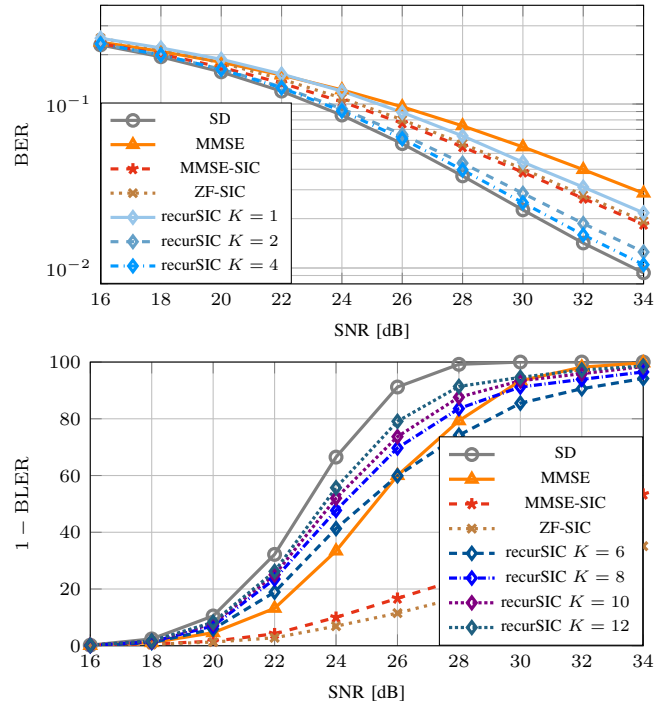


Fig. 6. Performance over TDL-B100 channel with 64QAM. Top: uncoded BER (hard-decision); bottom: relative throughput ($1 - \text{BLER}$) using soft-output.

- [7] L. G. Barbero and J. S. Thompson, "Fixing the complexity of the sphere decoder for MIMO detection," *IEEE Trans. Wireless Commun.*, vol. 7, no. 6, pp. 2131–2142, 2008.
- [8] R. Wang and G. Giannakis, "Approaching MIMO channel capacity with reduced-complexity soft sphere decoding," in *IEEE Wireless Commun. Netw. Conf.*, vol. 3, 2004, pp. 1620–1625 Vol.3.
- [9] C. Studer, A. Burg, and H. Bolcskei, "Soft-output sphere decoding: algorithms and VLSI implementation," *IEEE J. Sel. Areas Commun.*, vol. 26, no. 2, pp. 290–300, 2008.
- [10] D. L. Milliner, E. Zimmermann, J. R. Barry, and G. Fettweis, "A fixed-complexity smart candidate adding algorithm for soft-output MIMO detection," *IEEE J. Sel. Topics Signal Process.*, vol. 3, no. 6, pp. 1016–1025, 2009.
- [11] P. Wolniansky, G. Foschini, G. Golden, and R. Valenzuela, "V-BLAST: an architecture for realizing very high data rates over the rich-scattering wireless channel," in *URSI Int. Symp. Signals, Syst., Electron. Conf. Proceed.*, 1998, pp. 295–300.
- [12] M. Y. Daha, A. Sudhakaran, B. Babu, and M. U. Hadi, "Enabling intelligent 6G communications: A scalable deep learning framework for MIMO detection," *Telecom*, vol. 6, no. 3, 2025.
- [13] H. Ye and L. Liang, "On purely data-driven massive MIMO detectors," *IEEE Trans. Signal Process.*, vol. 73, pp. 3079–3093, 2025.
- [14] A. Askri and G. R.-B. Othman, "DNN assisted sphere decoder," in *IEEE Int. Symp. Inf. Theory (ISIT)*, 2019, pp. 1172–1176.
- [15] M. Mohammadkarimi, M. Mehrabi, M. Ardashri, and Y. Jing, "Deep learning-based sphere decoding," *IEEE Trans. Wireless Commun.*, vol. 18, no. 9, pp. 4368–4378, 2019.
- [16] D. Weon and K. Lee, "Learning-aided deep path prediction for sphere decoding in large MIMO systems," *IEEE Access*, vol. 8, pp. 70870–70877, 2020.
- [17] M. Yue, H. Wang, J. Qian, X. Huang, and X. Yuan, "Learned soft MIMO detection via search path selection and symbol distribution fitting," *IEEE Wireless Commun. Lett.*, vol. 13, no. 9, pp. 2377–2381, 2024.
- [18] N. Samuel, T. Diskin, and A. Wiesel, "Learning to detect," *IEEE Trans. Signal Process.*, vol. 67, no. 10, pp. 2554–2564, 2019.
- [19] H. He, C.-K. Wen, S. Jin, and G. Y. Li, "A model-driven deep learning network for MIMO detection," in *IEEE Global Conf. Signal Inf. Process. (GlobalSIP)*, 2018, pp. 584–588.
- [20] —, "Model-driven deep learning for MIMO detection," *IEEE Trans. Signal Process.*, vol. 68, pp. 1702–1715, 2020.
- [21] H. He, X. Yu, J. Zhang, S. Song, and K. B. Letaief, "Message passing meets graph neural networks: A new paradigm for massive MIMO systems," *IEEE Trans. Wireless Commun.*, vol. 23, no. 5, pp. 4709–4723, 2024.
- [22] K. Pratik, B. D. Rao, and M. Welling, "RE-MIMO: Recurrent and permutation equivariant neural MIMO detection," *IEEE Trans. Signal Process.*, vol. 69, pp. 459–473, 2021.
- [23] Y. Wei, M.-M. Zhao, M. Hong, M.-J. Zhao, and M. Lei, "Learned conjugate gradient descent network for massive MIMO detection," *IEEE Trans. Signal Process.*, vol. 68, pp. 6336–6349, 2020.
- [24] N. Shlezinger, R. Fu, and Y. C. Eldar, "DeepSIC: Deep soft interference cancellation for multiuser MIMO detection," *IEEE Trans. Wireless Commun.*, vol. 20, no. 2, pp. 1349–1362, 2021.
- [25] L. Li, T. Li, S. Fan, and X. Ji, "Residual-network enabled deep soft interference cancellation for MIMO detection without channel state information," in *IEEE 99th Veh. Technol. Conf (VTC2024-Spring)*, 2024, pp. 1–7.
- [26] I. Sim, Y. G. Sun, D. Lee, S. H. Kim, J. Lee, J.-H. Kim, Y. Shin, and J. Y. Kim, "Deep learning based successive interference cancellation scheme in nonorthogonal multiple access downlink network," *Energies*, vol. 13, no. 23, 2020.
- [27] Y.-S. Jeon, S.-N. Hong, and N. Lee, "Supervised-learning-aided communication framework for MIMO systems with low-resolution ADCs," *IEEE Trans. Veh. Technol.*, vol. 67, no. 8, pp. 7299–7313, 2018.
- [28] S. F. Qureshi, S. Damjancevic, E. Matus, P. v. d. Wolf, D. Utyansky, and G. Fettweis, "Low-complexity MIMO detection in 5G IoT: The box decoding approach," *J. Signal Process. Syst.*, vol. 97, pp. 1939–8115, 2025.
- [29] D. Wübben, R. Bohnke, V. Kuhn, and K.-D. Kammerer, "MMSE extension of V-BLAST based on sorted QR decomposition," in *IEEE 58th Veh. Technol. Conf. VTC 2003-Fall*, vol. 1, 2003, pp. 508–512.
- [30] B. Fesl, M. Baur, F. Strasser, M. Joham, and W. Utschick, "Diffusion-based generative prior for low-complexity MIMO channel estimation," *IEEE Wireless Commun. Lett.*, vol. 13, no. 12, pp. 3493–3497, 2024.
- [31] A. Vaswani, N. Shazeer, N. Parmar, J. Uszkoreit, L. Jones, A. N. Gomez, L. u. Kaiser, and I. Polosukhin, "Attention is all you need," in *Adv. Neural Inf. Process. Syst.*, vol. 30, 2017.